第 24 卷第 1 期
2008 年 1 月

无 机 化 学 学 报
CHINESE JOURNAL OF INORGANIC CHEMISTRY

Vol.24 No.1
43~46

简捷溶剂热技术制备纳米棒基 PbS 树枝晶

胡寒梅*,[1] 邓崇海[2] 朱绍峰[1] 李 燕[1]
([1]安徽建筑工业学院材料与化学工程学院,合肥 230022)
([2]合肥学院化学与材料工程系,合肥 230022)

摘要: 以氯化铅和硫氰酸钾为原料, 乙二醇为溶剂, 采用简捷溶剂热技术制备了半导体 PbS 纳米棒基树枝晶。粉体用 XRD、XPS、FESEM、TEM 和 ED 进行了表征。单个 PbS 树枝晶具有三维空间结构,由一个主干和四个相互垂直侧枝组成。主干长 2~10 μm,直径 150~300 μm,每组侧枝纳米棒相互平行,沿主干垂直生长,棒长 0.1~1.5 μm,直径 80~180 nm。并对生长过程进行了探讨。

关键词: PbS; 溶剂热技术; 树枝晶; 纳米棒
中图分类号: O611.4; O613.5 **文献标识码**: A **文章编号**: 1001-4861(2008)01-0043-04

Facile Solvothermal Route to Nanorod-based PbS Dendritic Crystals

HU Han-Mei*,[1] DENG Chong-Hai[2] ZHU Shao-Feng[1] LI Yan[1]
([1]*College of Materials and Chemical Engineering, Anhui Institute Architecture & Industry, Hefei* 230022)
([2]*Department of Chemistry and Materials Engineering, Hefei University, Hefei* 230022)

Abstract: Using $PbCl_2$ and KSCN as raw materials, nanorod-based PbS dendritic crystals were prepared in ethylene glycol (EG) under facile and mild solvothermal conditions. The as-prepared product was characterized by XRD, XPS, FESEM, TEM and ED. The individual PbS dendrite has three-dimensional (3D) structure with one trunk and four branches in a cross-like shape. The length of the trunk is in the range of 2~10 μm, with diameter of 150~300 nm. The branches have the length of 0.1~1.5 μm and the diameter of 80~180 nm, which grow in parallel with each other along directions perpendicular to the trunk. The possible growth mechanism is also discussed.

Key words: lead sulfide; solvethermal technique; dendritic crystal; nanorod

In recent years, inorganic semiconductors with hierarchical and complex dendritic superstructure at microscale have attracted a great deal of attention because of their intrinsic electronic, magnetic, photonic, and catalytic properties and potential applications in future devices[1~8]. As a kind of fractal structure, dendrites are generally formed by hierarchical self-assembly under non-quilibrium conditions [9,10], so they can provide a natural framework for the study of disordered systems.

As one kind of the most important lead mineral in the earths crust, lead sulfide (PbS) has attracted extensive attention because it is a naturally occurring semiconductor with small band gap energy (0.41 eV) and large exciton Bohr radius (18 nm)[11]. Solid-solution lead chalcogenide semiconductors are expected to be applied as tunable laser diodes that can operate in the

收稿日期:2007-09-10。收修改稿日期:2007-11-20。
国家自然科学基金(No.20501002),安徽省教育厅自然科学基金(No.2005KJ110,2006KJ159B),安徽省高校青年教师科研资助计划项目(No.2005jq1147zd,2006jq1228),安徽建筑工业学院博士启动基金(No.2004002)资助。
*通讯联系人。E-mail:hmhu@ustc.edu
第一作者:胡寒梅,女,31 岁,博士,副教授;研究方向:无机纳米材料的合成和性能研究。

mid-infrared wavelength region between 3×10^{-6} and 4×10^{-6} m. Blank and co-workers [12] have described the growth of PbS single crystals using the gel growth technique. García-Ruíz[13] has studied the growth of PbS single crystals in silica gels acidified with HCl and $HClO_4$. PbS with complex structures have attracted much attention because of their interesting morphologies and potential applications, such as dendritic and flower-like structures[14~17]. Recently, multi-level assemblies of PbS nanorods have been synthesized by an amino acid-mediated approach[18].

Herein, we report the growth of nanorod-based PbS dendritic crystals in the $PbCl_2$/KSCN/EG system under mild solvothermal conditions. The method is favorable to green environmental protection without use of any toxic organic solvents and surfactants. A possible formation mechanism of nanorod-based PbS dendritic c rystals is suggested.

1 Experimental

All chemicals (A. R.) were purchased from Shanghai Chemical Reagents Co. and used without further purification.

A typical preparation of nanorod-based PbS dendrites was as follows: 0.1 mmol $PbCl_2$ and 0.2 mmol KSCN were added into a 50 mL Telfon-lined stainless steel autoclave, which was then filled with ethylene glycol up to 90% of the total volume. The obtained reaction mixture was stirred for an additional 10 min. The autoclave was sealed and maintained at 200 ℃ for 12 h. After the reaction was completed, the resulting black solid products were filtered off, washed with absolute ethanol and distilled water for several times, and then finally dried in vacuum at 60 ℃ for 6 h.

The phase purity of the as-synthesized products was examined by XRD using a Philips XPert PRO SUPER X-ray diffractometer (40 kV, 50 mA) equipped with graphite monochromatized Cu-$K\alpha$ radiation (λ = 0.154 18 nm). The scan rate of 0.02° s^{-1} was applied and the patterns was recorded in the 2θ range of 20~70°. XPS spectra were recorded on a XR5 Monochromated X-ray Gun, using a non-monchromatized Al-$K\alpha$ X-ray as the excitation source to investigate the surface constituents. The morphology of the prepared products were observed on a field emission scanning electron microscope (JEOL-6300F, 15 kV). TEM image and SAED were obtained on a Hitachi Model H-800 transmission electron microscope with an accelerating voltage of 200 kV. The samples for TEM observation were dispersed in anhydrous ethanol under ultrasonication, and one drop of solution was deposited onto a carbon-coated copper grid before evaporating naturally.

2 Results and discussion

2.1 Characterization of the as-prepared products

A typical XRD pattern of the sample is shown in Fig.1. All the diffraction peaks can be indexed to face-centered cubic phase PbS with calculated cell constant a=0.594 0 nm, which is in agreement with the literature datum a=(0.593 6 nm (PDF2 05-0592)). No other impurities can be found in the pattern. The intense diffraction peaks suggest that the products are well crystallized.

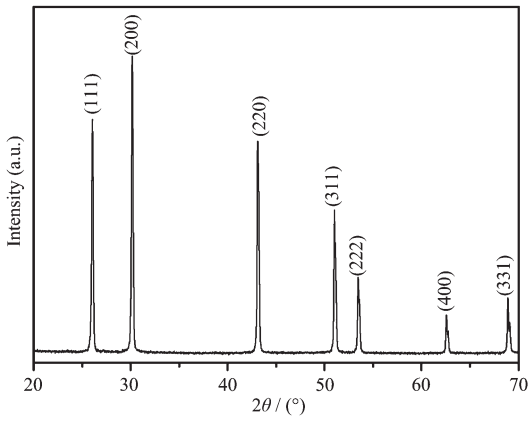

Fig.1 XRD pattern of the as-prepared products

Fig.2 gives the XPS spectra of the sample. A typical survey spectrum of PbS is shown in Fig.2a. The peaks of Pb and S can be clearly detected as well as those of C and O, which are attributed to the gaseous molecules from the air absorbed on the surfaces of the products. Fig.2b and 2c reveal the XPS spectra of Pb4f core level and S2p core level, respectively. The corresponding binding energy of Pb4$f_{7/2}$ and Pb4$f_{5/2}$ is 137.55 eV and 142.45 eV, respectively. Meanwhile, the peaks at 160.73 eV and 163.26 eV correspond to the binding energy of S2$p_{3/2}$, and the peaks at 161.92 eV

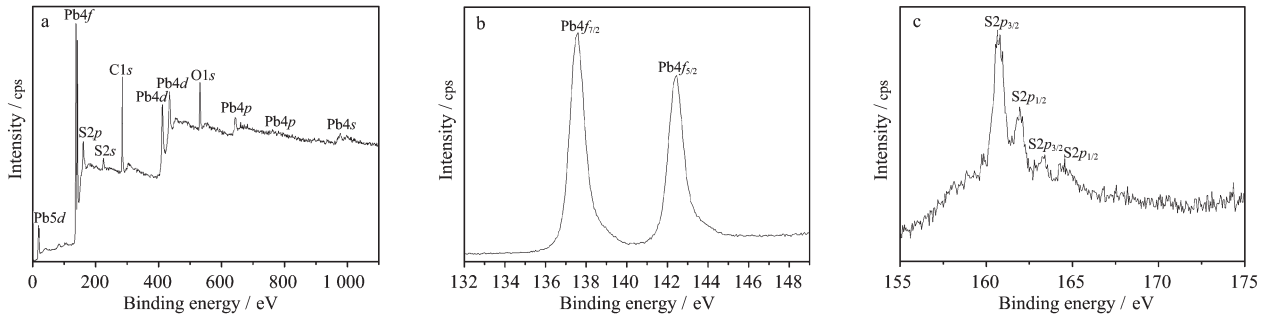

(a) typical survey spectrum, (b) Pb4f core level, (c) S2p core level

Fig.2　XPS spectra of the as-prepared products

and 164.67 eV are due to the binding energy of $S2p_{1/2}$.

Surface topographies of the as-prepared products are shown in Fig.3. FESEM images (Fig.3a-c) clearly show that the prepared PbS crystals mainly consist of nanorods arranged in dendritic structures. The individual PbS dendrite has three-dimensional (3D) structure with one trunk (long axis) and four branches (short axes) in a cross-like shape. On each dendritic structure, these rod-like branches grow in parallel with each other along directions perpendicular to the trunk (see magnified image inset in Fig.3a). The trunk is with a length of 2~10 μm and a diameter of 150~300 nm. The length of the nanorods is in the range of 0.1~1.5 μm, with diameter of 80~180 nm. A typical TEM image is shown in Fig.3d, indicating that the nanoscale PbS dendrites are indeed observed. The selected area electron diffraction (SAED) patterns (see image inset in Fig.3d) recorded from a nanorod in an individual PbS dendrite indicate the single crystalline nature of the PbS dendrite. Two typical diffraction spots can be indexed as the (200) and (020) lattice planes, respectively. Extensive investigations were also performed on more individual PbS dendrites with ED, the results of which demonstrate that as-synthesized nanorod-based PbS dendrites are composed of single crystals. In addition, the molar ratio of $PbCl_2$ to KSCN does not influence the morphology of PbS products. We performed a series of experiments under the same conditions except for molar ratio of Pb^{2+} to SCN^- (1∶1, 1∶4, 2∶1, 4∶1). Based on the FESEM observation, all these products are nanorod-based dendrite similar to Fig.3a. Note that in the 4∶1 (Pb^{2+}∶SCN^-) system, a large number of white unreacted $PbCl_2$ were existed in the products, which should be washed with hot water before characterization.

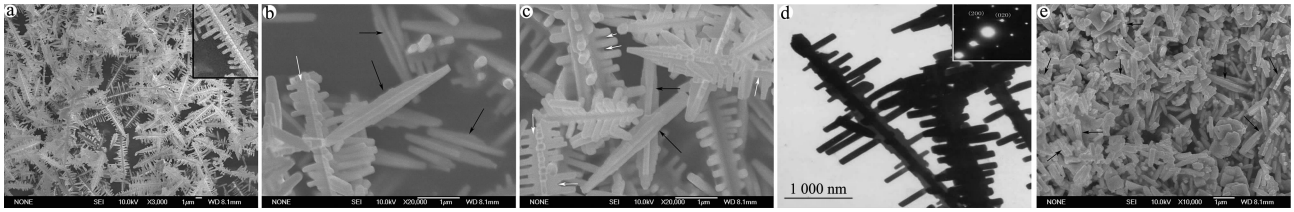

Fig.3　(a-c) FESEM images of the as-products prepared at 200 ℃ for 12 h; (d) TEM image of the as-products prepared at 200 ℃ for 12 h; (e) FESEM image of PbS products prepared at 200 ℃ for 3 h

2.2　Reaction mechanism

It is well known that SCN^- anion is a good linker ligand, which has been extensively studied in the field of coordination chemistry and supramolecular chemistry[18,19]. In our experimental system, $PbCl_2$ could not be dissolved in EG. When KSCN was added into the system, $PbCl_2$ powders was gradually dissolved and finally disappeared, implying the formation of $Pb_m(SCN)_n^{2m-n}$ coordination polymer. So, the two reactions are based on the formation of metal-thiocyanate polymer and then thermal decomposition to give the PbS products. The whole reaction process may be described as follows:

$$mPb^{2+} + nSCN^- \leftrightarrow Pb_m(SCN)_n^{2m-n} \quad (1)$$

$$4SCN^- + 9H_2O \rightarrow$$

$$CO_3^{2-} + S^{2-} + 3CO_2 + 3H_2S + 4NH_3 \quad (2)$$

$$Pb^{2+} + S^{2-} \rightarrow PbS \quad (3)$$

In addition, we have observed an interesting structure in the sample, i.e, orthogonal shuttle-like microstructure (indicated by black arrows in Figs.3b and c). When the reaction time is decreased to 3 h and keeping other conditions unchanged, much more developed or underdeveloped orthogonal shuttle-like structures are observed in the obtained sample (Fig.3e). It is suggested that the formation of nanorod-based dendrites may result from those orthogonal shuttle-like particles.

The experimental results imply that the formation of orthogonal shuttle-like PbS particles has a close relationship with the growth of nanorod-based PbS dendrites. We believe that the growth of nanorod-based PbS dendritic crystal mainly includes two steps: First, an orthogonal shuttle-like PbS crystal seed is produced by simultaneously growing out from the same nuclei along (100) and (010) 2D lattice plane of the PbS cubic unit cell ([001] direction is assumed as longitudinal axis). Second, the pre-obtained crystal seed serves as a good morphology-director for the subsequent growth of nanorod-based PbS dendrite. After a short period of rapid growth, the concentration of reactants is decreased, which could not satisfy the continuing growth of 2D fake-like nanostructure. It may lead to the further nucleation and 1D epitaxial growth proceeding at the growing fronts of the nanoflake. The marked white arrows in Figs.2b and c show that the bottoms of rod-shaped secondary branches are connected with each other on each dendritic structure, providing a supporting evidence for the proposed growth mechanism.

3 Conclusions

Nanorod-based PbS dendritic crystals have been prepared under a simple solvothermal condition in the absence of any surfactants or polymers. The characterization results (XRD, ED) show that the prepared 3D PbS dendrites crystallize very well. The experimental results reveal that the pre-obtained orthogonal shuttle-like PbS particle can serve as a good morphology-director for the subsequent growth of nanorod-based PbS dendritic crystal. The novel micropatterns could serve as building blocks to construct more complicated structures.

References:

[1] Sander L M. *Nature*, **1986**,**322**:789~793

[2] Ben-Jacob E, Garik P. *Nature*, **1990**,**343**:523~530

[3] Wang S Z, Xin H W. *J. Phys. Chem. B*, **2000**,**104**:5681~5685

[4] Li H, Zhu G Y, Huang X J, et al. *J. Mater. Chem.*, **2000**,**10**:693~696

[5] Tian Z R, Liu J, Voigt J A, et al. *Nano Lett.*, **2003**,**3**:89~92

[6] Xie S H, Zhou W Z, Zhu Y Q. *J. Phys. Chem. B*, **2004**,**108**:11561~11566

[7] Cao M H, Liu T F, Hu C W, et al. *Angew. Chem. Int. Ed.*, **2005**, **44**:4197~4201

[8] Wu Z C, Pan C, Yao Z Y, et al. *Cryst. Growth Des.*, **2006**,**6**:1717~1719

[9] Meakin P. *Phys. Rev. Lett.*, **1983**,**51**:1119~1122

[10]Lisiecki I, Albouy P A, Pileni M P. *Adv. Mater.*, **2003**,**15**:712~716

[11]Machol J L, Wise F W, Patel R C, et al. *Phys. Rev. B*, **1993**, **48**:2819~2822

[12]Blank Z, Brenner W, Okamoto Y. *Mater. Res. Bull.*, **1968**,**3**:555~562

[13]García-Ruíz J M. *J. Crystal Growth*, **1986**,**75**:441~446

[14]Kuang D B, Xu A W, Fang Y P, et al. *Adv. Mater*, **2003**,**15**:1747~1750

[15]Wang D B, Yu D B, Shao M W, et al. *J. Crystal Growth*, **2003**, **257**:384~389

[16]Ni Y H, Liu H J, Wang F, et al. *Cryst. Growth Des.*, **2004**,**4**:759~764

[17]Xu L Q, Zhang W Q, Ding Y W, et al. *J. Crystal Growth*, **2004**, **273**:213~219

[18]Lu Q Y, Gao F, Komarneni S. *Nanotechnology*, **2006**,**17**:2574~2580

[19]Bailey R A, Kozak S L, Michelse T W, et al. *Chem. Rev.*, **1971**,**6**:407~445